2800–2807 *Nucleic Acids Research, 1997, Vol. 25, No. 14*

Location of the internal ribosome entry site in the 5′ non-coding region of the immunoglobulin heavy-chain binding protein (BiP) mRNA: evidence for specific RNA–protein interactions

Qin Yang[+] and Peter Sarnow*

Department of Biochemistry, Biophysics and Genetics, University of Colorado Health Sciences Center, 4200 East Ninth Avenue, Denver, CO 80262, USA

Received March 31, 1997; Revised and Accepted May 28, 1997

ABSTRACT

The 220 nucleotide 5′ non-coding region (5′NCR) of the human immunoglobulin heavy chain binding protein (BiP) mRNA contains an internal ribosome entry site (IRES) that mediates the translation of the second cistron in a dicistronic mRNA in cultured mammalian cells. In this study, experiments are presented that locate the IRES immediately upstream of the start-site AUG codon in the BiP mRNA. Furthermore, crosslinking of thiouridine-labeled BiP IRES-containing RNA to cellular proteins identified the specific binding of two proteins, p60 and p95, to the 3′ half of the BiP 5′NCR. Interestingly, both p60 and p95 bound also specifically to several viral IRES elements. This correlation suggests that p60 and p95 could have roles in internal initiation of cellular and viral IRES elements.

INTRODUCTION

Most mRNA molecules in eukaryotic cells are translated by a scanning mechanism whereby 40S ribosomal subunits, carrying the initiator tRNA molecule and certain translational initiation factors, enter the mRNAs at or near their capped 5′ ends and subsequently scan the mRNA in a 5′ to 3′ direction until an appropriate AUG codon is encountered to start protein biosynthesis (1,2). However, several eukaryotic mRNAs have been identified that can recruit ribosomal subunits via internal ribosome entry site (IRES) sequence elements that are usually located within the 5′ non-coding regions (5′NCRs) of the mRNAs (reviewed in 3,4).

The existence of IRES elements was first noted in enteroviral (5) and cardioviral (6) RNA genomes, which are of positive-stranded polarity and lack 5′ terminal cap structures (7). It has long been known that cap-dependent translation of host cell mRNAs is inhibited in enterovirus-infected cells and it was thus unclear how viral mRNAs can be selectively translated in infected cells. It was subsequently found that eIF-4G (formerly known as p220 or eIF-4γ), a component of the cap binding protein complex eIF-4F, was cleaved in infected cells (8). As a consequence, translation initiation by the 5′ end-dependent scanning mechanism of capped cellular mRNAs is inhibited while translation by an internal ribosome entry mechanism of enteroviral mRNAs can proceed. This finding implies that internal initiation requires little intact eIF-4F. Because viral gene expression strategies usually usurp pathways that already exist in the host cells, quests were launched to identify cellular mRNAs that contain IRES elements. So far, a handful of IRES-containing cellular mRNAs have been described. Among those are the mRNAs encoding the human immunoglobulin heavy chain binding protein (BiP) (9), the *Drosophila melanogaster* Antennapedia protein (10), the human fibroblast growth factor protein (11), the human insulin growth factor protein (12) and the human eIF-4G protein (13). However, the exact locations of these IRES elements and the mechanism by which viral and cellular IRES elements are utilized still remain unknown.

Much effort has concentrated on the identification and characterization of factors that can modulate the function of IRES elements. Both general translation initiation factors and novel nuclear proteins have been identified which stimulate internal initiation. Initiation factor eIF-4A has been shown to be essential in internal initiation, because dominant negative mutations in eIF-4A inhibit both cap-dependent and internal initiation-dependent translation in mammalian cells (14). Furthermore, evidence is accumulating that the C-terminus of factor eIF-4G, which is generated by proteolysis in enterovirus-infected cells, as mentioned above, enhances internal ribosome binding. Specifically, eIF-4G is cleaved in infected cells to yield two major cleavage products: an N-terminal 130 kDa cleavage product which remains bound to the cap binding protein eIF-4E, and a C-terminal 100 kDa cleavage product which remains associated with factors eIF-4A and eIF-3 (15,16). Recently, it has been shown that the eIF-4G$_{C\text{-}terminal}$/eIF-4A/eIF-3 complex stimulates the translation of IRES-containing mRNAs in cell-free translation systems (16,17). Whether the eIF-4G$_{C\text{-}terminal}$/eIF-4A/eIF-3 complex

*To whom correspondence should be addressed at present address: Department of Microbiology and Immunology, Stanford University School of Medicine, Stanford, CA 94305, USA. Tel: +1 415 498 7076; Fax: +1 415 498 7147; Email: psarnow@leland.stanford.edu

[+]Present address: School of Pharmacy, University of Colorado Health Sciences Center, 4200 East Ninth Avenue, Denver, CO 80262, USA

stimulates IRES elements in infected cells and by what mechanism is not known.

Using gel-shift and ultraviolet crosslinking assays, complexes between several different nuclear proteins and IRES elements have been identified. Of these, the La autoantigen (18,19) and the polypyrimidine tract binding protein PTB (20,21) have been shown to be required for efficient internal ribosome entry in polioviral (22) and encephalomyocarditis viral (23,24) IRES elements, respectively. Interestingly, neither La nor PTB seems to specifically interact with the cellular BiP IRES (unpublished observation). However, this may not be too surprising because even different viral IRES elements have different requirements for PTB (24). This study shows that two cellular proteins, p60 and p95, specifically interact with the BiP 5′NCR as well as with several viral IRES elements.

MATERIALS AND METHODS

Plasmid construction

Plasmids pT7BiPLUC, pSV$_A$CAT/ICS/LUC, pSV$_A$CAT/BiP/LUC, pSV$_A$CAT/ED/LUC and pSV$_A$(hairpin)CAT/BiP/LUC plasmids have been described (9,25). Plasmid pSV$_A$CAT/BiP$_{Nru\text{-}AUG}$/LUC was derived from pSV$_A$CAT/BiP/LUC by inserting an *Nco*I linker CATGCCATGGCATG (the AUG triplets are underlined) at the *Nru*I site located at position 53 in the BiP 5′NCR. Plasmid pT7BiP$_{S\text{-}N}$LUC was constructed by the following method: pT7BiPLUC was first digested with *Hin*dIII, the protruding ends were repaired with Klenow enzyme, and the treated DNA was digested with *Nco*I. The large 5.3 kb DNA fragment was then purified by agarose gel electrophoresis. Separately, an *Sma*I–*Nco*I fragment, containing nucleotides (nt) 130–220 of the BiP 5′NCR, was isolated from pT7BiPLUC digested with *Sma*I and *Nco*I. The two fragments were then ligated to give rise to the plasmid pT7BiP$_{S\text{-}N}$LUC. Plasmid pT7BiPX-NLUC was constructed by the same strategy: pT7BiPLUC was first digested with *Xba*I, treated with Klenow enzyme, and digested with *Nco*I. The 129 bp BiP 5′NCR fragment was ligated to the 5.3 kb vector as described above. Plasmid pT7BiP$_{60\text{-}165}$LUC was constructed by polymerase chain reaction (PCR) using two deoxyoligonucleotides: one containing a *Sal*I-site attached to nucleotides representing positions 60–80 of the BiP 5′ NCR (5′-GTCGACATGAGAGGGAAGCGCCGCG-GCC-3′) and one representing an *Nco*I-linker attached to the complement of nt 143–165 of the BiP 5′ NCR (5′-CCATGGA-CACAGCGCAATTTCGACTTGCAG-3′). The amplified fragment was cloned into plasmid pGEM-T (Promega Biotec.), giving rise to plasmid pT7BiP$_{60\text{-}165}$. This plasmid was digested with *Sal*I, treated with Klenow enzyme, and then cut with *Nco*I. The *Sal*I$_{klenow}$–*Nco*I fragment was ligated to the 5.3 kb pT7LUC fragment as described above to yield pT7BiP$_{60\text{-}165}$. Plasmid pT7BiP$_{N\text{-}S}$LUC was constructed by ligation of the 5.3 kb fragment, obtained after digestion of plasmid pT7BiPLUC with *Nru*I and *Nco*I, to a 91 bp fragment obtained after digestion of plasmid pT7BiPLUC with *Sma*I and *Nco*I. Plasmid pT7BiP$_{N\text{-}H}$ LUC was constructed by ligating the 5.3 kb *Nru*I–*Nco*I fragment (see above) to a 59 bp fragment obtained after cleavage of plasmid pT7BiPLUC with *Hin*PI, followed by treatment with Klenow and *Nco*I. Plasmid pT7BiP$_{H\text{-}N}$LUC was constructed by the ligation of the *Hin*PI$_{klenow}$–*Nco*I fragment (see above) to the 5.3 kb pT7BiPLUC/*Hin*dIII$_{klenow}$–*Nco*I fragment (see above). Plasmid pSV$_A$CAT/BiP$_{Nru}$/LUC was constructed by the following method: plasmid pSV$_A$CAT/BiP/LUC (9) was digested with various enzymes and the 6.6 kb *Sal*I–*Bst*EII fragment, the *Sal*I–*Nru*I fragment containing nt 1–53 of the BiP 5′NCR and the 605 bp *Nco*I$_{klenow}$–*Bst*EII fragment were isolated. The three fragments were ligated to give rise to the plasmid pSV$_A$CAT/BiP$_{Nru}$/LUC. Plasmid pSV$_A$CAT/BiP$_{Xba}$/LUC was constructed using the same strategy. Three fragments were obtained from digested pSV$_A$CAT/BiP/LUC plasmids: a 6.6 kb *Sal*I–*Bst*EII fragment, a *Sal*I–*Xba*I$_{klenow}$ fragment containing nt 1–91 of the BiP 5′NCR and a 605 bp *Nco*I$_{klenow}$–*Bst*EII were ligated to yield plasmid pSV$_A$CAT/BiP$_{Xba}$/LUC. To obtain the pSV$_A$CAT/BiP$_{60\text{-}165}$/LUC plasmid, the *Sal*I–*Nco*I fragment was isolated from pT7BiP$_{60\text{-}165}$ (see above) and was ligated to the 6.6 kb *Sal*I–*Bst*EII and the 605 bp *Nco*I–*Bst*EII fragments, both obtained from digestions of plasmid pSV$_A$CAT/BiP/LUC. Plasmid pSV$_A$CAT/BiP$_{Sma}$/LUC was constructed similarly to pSV$_A$CAT/BiP$_{Nru}$/LUC (see above), except that the fragment containing the BiP 5′NCR sequence was replaced with the *Sal*I–*Sma*I (BiP$_{1\text{-}129}$) fragment. Constructions of plasmids pSV$_A$CAT/BiP$_{S\text{-}N}$/LUC, pSV$_A$CAT/BiP$_{N\text{-}S}$/LUC, pSV$_A$CAT/BiP$_{N\text{-}H}$/LUC and pSV$_A$CAT/BiP$_{H\text{-}N}$/LUC were accomplished by three-fragment ligation methods. Fragment 1 contained the 6.6 kb *Sal*I$_{klenow}$ –*Bst*EII fragment isolated from digested pSV$_A$CAT/BiP/LUC. Fragment 2 contained the 605 bp *Nco*I–*Bst*EII fragment, also obtained from digested pSV$_A$CAT/BiP/LUC. The third fragment varied; the *Sma*I–*Nco*I (BiP$_{130\text{-}220}$) fragment from pSV$_A$CAT/BiP/LUC was used for the construction of pSV$_A$CAT/BiP$_{S\text{-}N}$/LUC; the *Hin*dIII$_{klenow}$–*Nco*I fragment from pT7BiP$_{N\text{-}S}$LUC (see above) was used for the construction of pSV$_A$CAT/BiP$_{N\text{-}S}$/LUC; the *Hin*dIII$_{klenow}$–*Nco*I fragment from pT7BiP$_{N\text{-}H}$LUC (see above) was used for the construction of pSV$_A$CAT/BiP$_{N\text{-}H}$/LUC, and the *Hin*PI$_{klenow}$–*Nco*I fragment from pT7BiPLUC was used for the construction pSV$_A$CAT/BiP$_{H\text{-}N}$/LUC. In addition, versions of plasmids pSV$_A$CAT/BiP$_{Nru}$/LUC, pSV$_A$CAT/BiP$_{Xba}$/LUC, pSV$_A$CAT/BiP$_{60\text{-}165}$/LUC pSV$_A$CAT/BiP$_{N\text{-}S}$/LUC, pSV$_A$CAT/BiP$_{N\text{-}H}$/LUC and pSV$_A$CAT/BiP$_{H\text{-}N}$/LUC were constructed that could directed the synthesis of dicistronic mRNAs which contained stable hairpin structures upstream of the CAT coding regions (9).

In vivo translational analyses

HeLa cells were transfected with 5 µg of plasmid DNA per 100 mm tissue culture dish (2×10^6 cells) by a calcium phosphate transfection procedure as described (26). Cell extracts were prepared 48 h after transfection and analyzed for chloramphenicol acetyltransferase activity using a phase-extraction method (26) and for luciferase activity according to De Wet *et al.* (27).

Isolation and analysis of RNA

Poly(A$^+$) mRNAs were isolated using the Dynabeads mRNA DIRECT kit (Dynal). Briefly, 1 ml of lysis/binding buffer was added to a frozen HeLa cell pellet (2×10^6) to induce cell lysis. The cell lysate was mixed with 1 mg of Dynabeads Oligo $(dT)_{25}$ in an Eppendorf tube at room temperature for 5 min. The beads were then separated from the supernatant by placing the tube in a magnetic field (Dynal MPC). After washing the beads three times, the bound mRNAs were eluted from the beads by addition of 10 µl of elution solution and heating at 65 °C for 2 min. Isolated mRNAs were analyzed by Northern hybridization as described (26).

In vitro RNA synthesis

RNA molecules were synthesized in the presence of [^{32}P]CTP (800 Ci/mmol) and 4-thioUTP by T7 RNA polymerase as described previously (28) with some modifications. After the transcription reaction, unincorporated nucleotides were removed by two successive ammonium acetate/ethanol precipitations. The integrity of the transcripts was analyzed by denaturing polyacrylamide gel electrophoresis.

Unlabelled competitor RNAs were synthesized according to standard protocols (Promega Biotec.). After treatment with RNase-free DNase RQ1 (Promega Biotec.), the RNAs were extracted with phenol–chloroform. Unincorporated nucleotides were removed by spin column chromatography with Sephadex G-25 followed by ethanol precipitation. RNA concentrations were calculated by measuring the A_{260} (40 µg/ml/A_{260} unit). The integrity of the RNAs was analyzed by gel electrophoresis.

To synthesize full-length BiP 5′NCRs, pT7BiPLUC was linearized with *Nco*I and used as template for transcription. To synthesize RNAs containing the iron-responsive element (IRE), plasmid I-12.CAT (kindly provided by Dr Matthias W.Hentze, EMBL Laboratories) was linearized with *Pvu*II and used as template for RNA synthesis. P4 RNA was transcribed from plasmid pGEM4 (Promega Biotec.), linearized with *Nhe*I. RNAs representing particular regions of the BiP 5′NCR were transcribed either from pT7BiPLUC plasmid, linearized with appropriate restriction endonucleases (*Nru*I, *Xba*I or *Sma*I) or from various BiP 5′NCR deletion mutant-containing plasmids (see plasmid construction), linearized with appropriate enzymes (*Sma*I for $BiP_{X\text{-}S}$ RNA and *Nco*I for other RNAs). The 5′NCR of hepatitis C virus (HCV) was transcribed from plasmid 5HcCAT (29), linearized with *Nco*I. The 5′NCR of encephalomyocarditis virus (EMCV) was transcribed from plasmid pCi-LUC plasmid (30), linearized with *Sma*I. Transcribed RNA contains nt 260–834 of the EMCV 5′NCR linked to 55 nt of the luciferase coding region. The 5′NCR of type 1 poliovirus mRNA was transcribed from plasmid p X (30), linearized with *Sma*I. This RNA species contains the full-length polioviral 5′NCR linked to 55 nt of the luciferase coding region. The 5′NCR of the β-globin mRNA was transcribed from plasmid pLUC (30), linearized with *Sma*I. Transcribed RNA species contain the full-length β-globin 5′NCR linked to 55 nt of the luciferase coding region.

Preparation of HeLa cell extracts

HeLa extracts were prepared by both the Nonidet P-40 lysis method as described (31) and the douncing method of Dignam *et al.* (32,33). The nuclear pellets from these preparations were used as the source of the nuclear extract as described (32,33). The crude nuclear extracts were fractionated by successive ammonium sulfate precipitation (0–20, 20–40, 40–60, 60–80 and 40–80%) according to Englard and Seifert (34).

Ultraviolet crosslinking assay

Ultraviolet (UV) crosslinking assays were carried out as described (28) with some modifications. Samples containing 20 µg of protein (crude HeLa cell extracts or ammonium sulfate fractionated samples) were incubated with the 4-thioU-containing radiolabeled RNA (4×10^5 c.p.m., 1 nM for the full-length BiP 5′NCR) in the absence or presence of unlabelled competitor RNA in a 30 µl reaction volume (10 mM HEPES–NaOH pH 7.4, 3 mM $MgCl_2$, 1.3 mM ATP, 5 mM creatine phosphate, 1 mM DTT, 100 mM KCl and 6% glycerol) for 15 min at 30°C. The reaction mixtures were then irradiated at 312 nm UV light in a Stratalinker model 1800 (Stratagene) for 30 min at 4°C. After irradiation, the samples were digested with 0.2 mg/ml pancreatic RNase A (US Biochemicals) for 20 min at 37°C. The crosslinked RNA–protein complexes were then analyzed after separation in 10% SDS-containing polyacrylamide gels followed by autoradiography.

RESULTS

The BiP 5′NCR directs the translation of a second cistron in a dicistronic mRNA by an internal initiation and not by a reinitiation mechanism

The 5′NCR of human BiP mRNA is 220 nt in length (35) and has been shown to contain an IRES (9). This conclusion was obtained from studying the translation of dicistronic mRNAs containing the BiP 5′NCR inserted between the two cistrons. It was observed that translation of the second cistron occurred independently of the translation of the first cistron (9). Specifically, the translation of the first cistron was inhibited in the presence of a stable hairpin structure at the 5′ end. Translation of the second cistron from the hairpin-containing dicistronic mRNA was not affected which indicted that the BiP 5′NCR functions as an IRES element and not as an RNA element that can promote reinitiation events with high frequency (9).

More recently, it has been shown that mRNAs containing hairpin structures at their very 5′ end (i.e. as few as 5 nt downstream of the cap structure) were not translated although such mRNAs could be detected in 43S preinitiation complexes (36). Therefore, hairpin-containing dicistronic mRNAs could, in principle, have bound 43S ribosomal complexes which could have been transferred to sequences located upstream of the BiP 5′NCR. As result, ribosomal subunits or ribosomes could have traversed the BiP 5′NCR and translated the second cistron by a reinitiation mechanism. To examine this possibility, three AUG triplets were inserted at position 53 of the BiP 5′NCR. The first AUG codon, which is out-of frame with the start-site AUG codon of the second cistron (luciferase), is followed by an open reading frame which terminates at position 89 in the BiP 5′NCR. The second AUG codon is in frame with the start-site AUG codon of BiP, thereby extending the BiP open reading frame. The third AUG codon is out-of frame with the start-site AUG codon and is followed by a short open reading frame that terminates at position 60 in the BiP 5′NCR. Transfection of plasmids encoding dicistronic transcripts with wild-type or AUG-burdened BiP 5′NCRs into cultured HeLa cells resulted in the synthesis of very similar amounts of luciferase (Fig. 1). In contrast, unrelated ED sequences mediated the translation of the second cistron very poorly (Fig. 1). Thus, the second cistron in BiP 5′NCR-containing dicistronic mRNAs was not synthesized by a reinitiation mechanism. Instead, the BiP 5′NCR functions as an IRES in these dicistronic mRNAs.

Location of the IRES in the BiP 5′NCR

To locate the internal ribosome entry in the 5′NCR of the BiP mRNA, various parts of the BiP 5′NCR were inserted into a dicistronic plasmid vector. Plasmids were transfected into HeLa

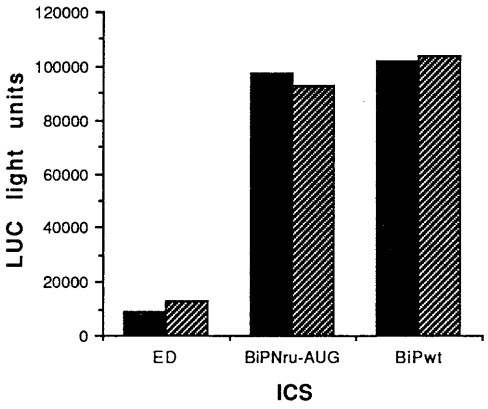

Figure 1. Internal initiation of translation mediated by the BiP 5′NCR lacking or containing upstream AUGs. Three upstream AUGs were created by insertion of an *Nco*I linker at the *Nru*I site (nt 53) of the BiP 5′NCR as described in Materials and Methods. Three dicistronic plasmids: pSVCAT/BiP/LUC, pSV/CAT/ED/LUC and pSVCAT/BiP$_{Nru\text{-}Aug}$/LUC were transfected into HeLa cells. Luciferase (LUC) activity from two separate experiments is shown after normalizing to the amount of chloramphenicol transacetylase (CAT) activity in the same extracts. The first cistron in the dicistronic mRNA encodes CAT. ICS denotes the various intracistronic spacer regions.

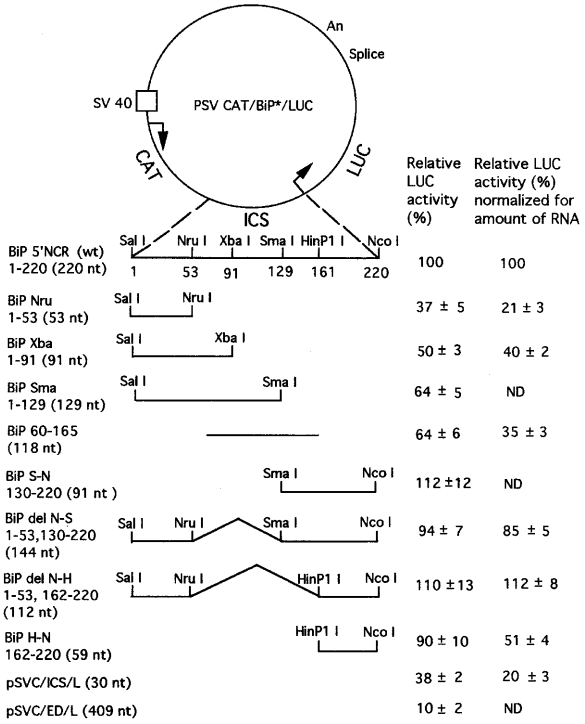

Figure 2. Schematic representation of the dicistronic plasmids containing different regions of the BiP 5′NCR in the intracistronic spacer region (ICS) and their efficiency in directing internal ribosome binding. The plasmids were transfected into HeLa cells, soluble proteins were extracted and enzyamtic assays were carried out as described in Materials and Methods. Relative luciferase activity is displayed in two ways. (i) The CAT activity was used as an internal control for normalizing the LUC activity from the same extracts. The normalized LUC activity (shown on the right) from extracts transfected with different plasmids was then compared to the LUC activity obtained from extracts transfected with dicistronic plasmids containing the full-length BiP 5′NCR in the ICS. (ii) The steady state levels of dicistronic mRNAs shown in Figure 3 were used as internal control for normalizing the LUC activity.

cells and the amounts of expression of the first CAT cistron and the second luciferase (LUC) cistron were determined. Figure 2 lists the relative efficiencies of luciferase expression from the second cistron of the dicistronic mRNAs, mediated by the various BiP 5′NCRs. Compared to the entire BiP 5′NCR (100%), control sequences ED (10%) functioned poorly as IRES elements. RNA sequences containing only the 3′ half of the BiP 5′NCR (S-N, del N-S, del N-H, H-N) functioned as efficiently as the entire BiP 5′NCR as IRES elements. However, control dicistronic sequences (ics), which contain a short polylinker between the two cistrons, and sequences 1–53 (Nru) functioned quite efficiently in mediating second cistron translation. Of course, in any of these dicistronic mRNAs, second cistron translation could have resulted from broken, uncapped mRNAs. Alternatively, short sequence elements derived from the BiP 5′NCR, which lacks AUG triplets, such as the Nru RNA element or the ics RNA element, could have mediated luciferase translation by a reinitiation mechanism. Such a mechanism has been shown to operate in mammalian cells when intracistronic spacer sequences are small (37). To examine these possibilities, sequences which can fold into a stable RNA hairpin were inserted into the 5′NCR of the CAT cDNA (9). After transfection of such hairpin-encoding dicistronic plasmids into HeLa cells, extracts were prepared and the dicistronic mRNAs were analyzed by Northern analysis (26). Figure 3 shows that all dicistronic mRNA species remain largely intact in extracts prepared from transfected cells. Next, luciferase was measured in the same extracts (Cat activity could not be detected) and displayed after quantification of the dicistronic mRNA and normalization to actin mRNA, to correct for loss of RNA during manipulations of the samples. The corrected luciferase activities are displayed in Figure 2 (right column). The results showed that BiP 5′NCR sequences 1–53, 130–220 (delN-S) or 1–53, 162–220 (delN-H) mediated internal initiation with much higher efficiency than sequences 1–53 (Nru) or control (ics) sequences. The drop in IRES efficiency of fragment H-N in hairpin-containing dicistronic mRNA indicates that H-N sequences present in non-hairpin mRNAs may promote reinitiation events. Curiously, delN-H sequences more efficiently mediated internal initiation than H-N (162–220) sequences after normalization. While there is no obvious explanation for these data, RNA folding analyses have shown that the BiP 5′NCR can be folded into a predicted Y-shaped structure (38,39), and that the presence of the first 53 nt favor the formation of the predicted Y-shaped structure mediated by sequences 162–220 (data not shown). If the Y-shaped structure of the BiP 5′NCR is an important element of its IRES activity, than the 5′ proximal nucleotides in BiP mRNA could contribute to the formation of an efficient IRES. Overall, sequences which mediate efficient internal initiation are located between nucleotides 129 and 220, i.e. the 3′ end of the BiP 5′NCR.

Identification of specific BiP 5′NCR–protein complexes

An ultraviolet crosslinking assay was employed to detect specific complexes that could form between the BiP 5′NCR and cellular factors. As described in Materials and Methods, radiolabeled and thio-uridine containing BiP 5′NCR elements were incubated with unfractionated or ammonium sulfate-fractionated extracts and irradiated at 302 nm. Crosslinked complexes were visualized by phosphoimaging after RNase digestion and separation on SDS–

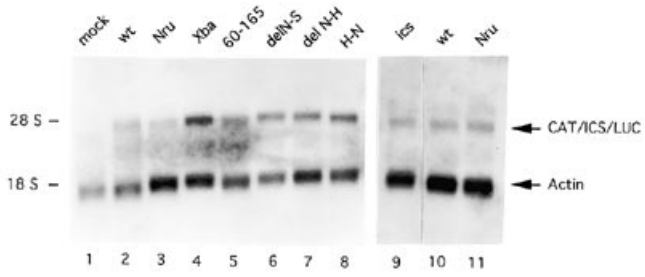

Figure 3. Analyses of the mRNAs expressed from dicistronic hairpin-CAT/ICS/LUC plasmids. Various PSVCAT/ICS/LUC plasmids that contained a stable RNA hairpin upstream of CAT coding region were constructed as described in Materials and Methods. HeLa cells were transfected with the plasmids and harvested 2 days after transfection. Half of the cells from each transfection was used for mRNA isolation; the other half was used for soluble protein preparation. The mRNAs were analyzed by Northern blot hybridization using radiolabeled RNAs that hybridized to luciferase or actin sequences (see Materials and Methods). An autoradiograph of the blotted gel is shown. The various sequences present in the ICS of the dicistronic molecules are shown on the top of each lane. Lane 1, mock transfection. Lanes 2 and 10, full-length BiP 5′NCR. Lanes 3–8, different deletion mutants of the BiP 5′NCR. Lane 9, control with no added sequences in the ICS. Lane 11, repetition of experiment shown in lane 3. The migration of 18S and 28S ribosomal RNA are denoted on the left. The bands representing the dicistronic (CAT/ICS/LUC) and the actin mRNA are indicated on the right. The intensities of the CAT/ICS/LUC and actin bands were quantitated by phosphorimaging. The relative amount of the dicistronic mRNA was determined by normalization to the actin mRNA in the same lane. Then, luciferase activity in the same extract was expressed as the percentage of luciferase activity obtained from the same number of cells transfected with CAT-BiP 5′NCR-LUC encoding plasmid.

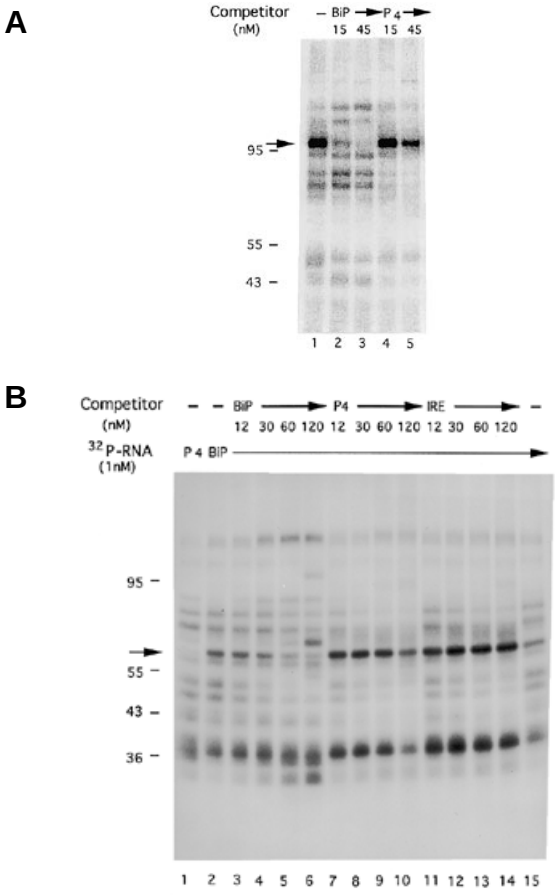

Figure 4. Competition of p95– (**A**) and p60–BiP 5′NCR (**B**) complex formation with unlabeled RNAs. Radiolabeled BiP 5′NCR (1 nM) was used in the crosslinking experiments with increasing amounts of unlabeled competitor RNAs. (**A)** Binding competition with p95–BiP 5′NCR complexes. 40–80% ammonium sulfate-fractionated nuclear extracts were used. Lane 1, no competitor. Lanes 2 and 3, 15 and 45 nM of unlabeled BiP 5′NCR as competitor. Lanes 4 and 5, P4 RNA as competitor. A phosphorimage of the SDS–polyacrylamide gel is shown. (**B)** Binding competition with p60–BiP 5′NCR complexes. 20–40% ammonium sulfate-fractionated nuclear extracts were used. Lane 1, crosslinking to radiolabeled P4 RNA. Lanes 2–15, crosslinking to radiolabeled BiP 5′NCR in the absence of competitor RNA (lanes 2 and 15), or presence of increasing amount of various competitor RNAs (lanes 3–14). Competitor RNAs were BiP 5′NCR (BiP), P4 or the iron responsive element RNA (IRE) as indicated. An autoradiograph of the gel is shown. Protein molecular weight markers (kDa) are shown on the left. The arrow indicates the migration of p95 (A) and p60 (B), respectively.

polyacrylamide gels. Numerous protease-sensitive factors, present in both nuclear and cytoplasmic fractions, could be crosslinked to the BiP 5′NCR (data not shown). However, a 95 kDa (p95) protein (Fig. 4A, lane 1), present in the 80% ammonium sulfate precipitate, and a 60 kDa (p60) protein (Fig. 4B, lane 2), present in the 40% ammonium sulfate precipitate, could be specifically crosslinked to the BiP 5′NCR. The presence of p95 and p60 in different ammonium sulfate fractions could be due to the association of these proteins in complexes which display different solubilities in ammonium sulfate. Figure 4A shows that addition of a 15-fold molar excess of unlabeled BiP 5′NCR RNA to the binding reaction greatly abolished the formation of BiP 5′NCR–p95 complexes (lane 2). In contrast, this effect was not observed by the addition of the same amount of a control P4 RNA which has similar length and nucleotide composition as the BiP 5′NCR (lane 4). Similarly, a 60-fold molar excess of unlabeled BiP 5′NCR in the reaction inhibited the formation of BiP 5′NCR–p60 complexes (Fig. 4B, lane 5), while the presence of similar amounts of P4 RNA had no effect on binding of p60 to the BiP 5′NCR (lane 9). The presence of non-BiP competitor RNAs actually enhanced the binding of p60 to BiP RNA (lanes 7–14); this could be due to inhibition of formation of p60–BiP RNA complexes by non-specific RNA binding proteins that have higher affinity for non-BiP competitor RNAs. Importantly, the iron-responsive element (IRE) (40,41), a highly structured RNA, did not abolish the formation of BiP 5′NCR–p60 (lanes 11–15) or BiP 5′NCR–p95 (Fig. 6B, lane 5) complexes. This finding supports the idea that p60 and p95 are RNA binding proteins that interact with specific RNA sequences or RNA structures in the BiP 5′NCR.

Delineation of the binding sites of p95 and p60 in the BiP 5′NCR

The binding sites for p95 and p60 in the BiP 5′NCR were determined by binding of partially purified proteins (see Materials and Methods) to various regions of the BiP 5′NCR. Figure 5A shows that p95 bound preferentially to sequences representing the 3′ half of the BiP 5′NCR. For example, all RNAs that contained sequences 3′ of nt 129 (lanes H-N, X-N, S-N and delN-H; see Fig. 2 for a detailed map) bound p95 with an efficiency comparable to that of the full-length BiP 5′NCR (lanes 1, 6 and 10). In contrast, sequences that contained the 5′ proximal 53 or 91 nt of the BiP 5′NCR (lanes Nru and Xba, respectively; see Fig. 2 for a detailed map) bound poorly to p95. RNA

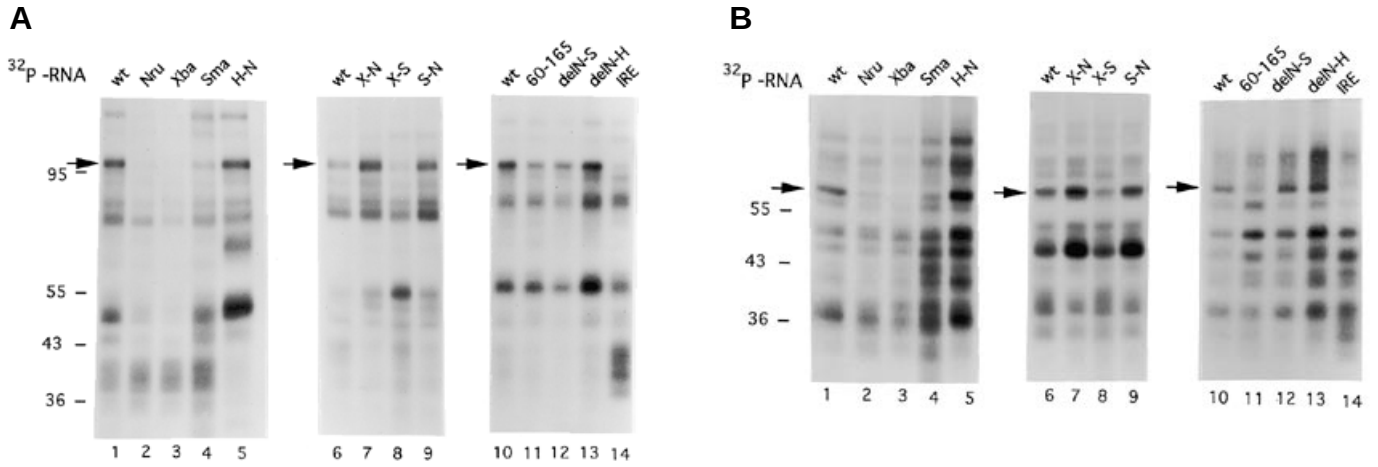

Figure 5. Mapping of the binding sites of p95 and p60 in the BiP 5′NCR. Different radiolabeled regions of the BiP 5′NCR were synthesized as described in Materials and Methods, and used in protein crosslinking assays. (**A)** Binding of p95. Lanes 1, 6 and 10: full-length BiP 5′NCR (220 nt). Lanes 2–5, 7–9, 11–13, different regions of the BiP 5′NCR as indicated on the top of each lane. Lane 14, IRE RNA. (**B)** Binding of p60. The samples are in the same order as in (A). Protein molecular weight markers (kDa) are shown on the left. Phosphorimages of the SDS–polyacrylamide gels are shown. The arrow indicates the migration of p95 (**A**) and p60 (**B**), respectively.

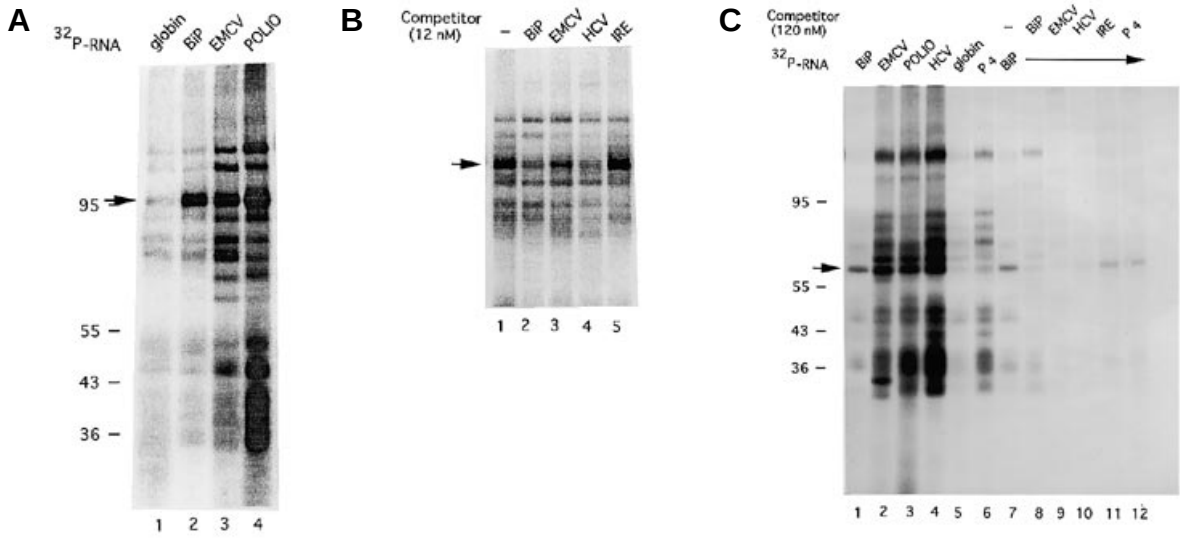

Figure 6. Binding of p95 and p60 to viral IRES elements. (**A)** Binding of p95 to viral IRES elements. The 5′NCRs of β-globin, BiP, encephalomyocarditis virus (EMCV) and poliovirus (POLIO) mRNAs were crosslinked to 40–80% of ammonium sulfate-fractionated nuclear extracts, processed as described in Materials and Methods and analyzed in an SDS–polyacrylamide gel. A phosphorimage of the gel is shown. The various radiolabeled RNA molecules are indicated on the top of each lane. Protein molecular weight markers (kDa) are shown on the left. The arrow indicates the p95 band. (**B)** Binding competititon of p95–BiP 5′NCR complexes, formed with 1 nM labeled BiP 5′NCR, by various unlabeled RNAs. Lane 1, no competitor. Lanes 2–4, the 5′ NCR of BiP, EMCV or HCV mRNA as competitors. A phosphorimage of the gel is shown. The arrow indicates the p95 band. (**C)** Binding of p60 to viral IRESes shown in direct crosslinking and competition experiments. Lanes 1–6, crosslinking of p60 (20–40% ammonium sulfate-precipitated nuclear extract) to 1 nM of various radiolabeled RNAs, denoted on the top of each lane. Lanes 7–12, binding competition. Radiolabeled BiP 5′NCR (1 nM) was incubated with the protein sample in the absence or presence of various unlabelled RNAs as competitor. Lane 7, no competitor. Lanes 8–12, the 5′ NCR of BiP, EMCV, HCV mRNAs or IRE and P4 RNAs as competitors. An autoradiograph of the gel is shown. Protein molecular weight markers (kDa) are shown on the left. The arrow indicates the migration of p60.

molecules that contained nt 1–129 (Sma) or 60–165 bound little but detectable amounts of p95, indicating that sequences located in the middle of the Bip 5′NCR have weak affinity for p95. Lane 14 shows that several proteins, including a 50 kDa polypeptide, could be crosslinked to both IRE-containing RNAs and RNAs representing the various BiP 5′NCRs; in contrast, the IRE did not bind significant amounts of p95.

The binding of p60 to BiP 5′NCR-containing RNA molecules is shown in Figure 5B. The binding site for p60 seems to be similar to the binding site for p95, as discussed above, with the

exception that fragment 60–165 bound p60 very poorly (lane 11). Overall, these direct binding experiments indicate that both p95 and p60 bind to the 3′ half of the 5′NCR of BiP mRNA.

Table 1. Competition of various segments of the BiP 5′NCRs with binding of p95 or p60 to full-length BiP 5′NCR

Exp.	Competitor RNA	Concentration of competitor RNA (nM)[a]		Fold increase over full-length 5′NCR BiP	
		p95	p60	p95	p60
1	BiP 5′NCR	35	68	1	1
	Nru	350[b]	1000[b]	10	15
	H-N	ND	85	ND	1.2
2	BiP 5′NCR	15	43	1	1
	delN-S	15	72	1	1.7
	delN-H	18	80	1.2	1.9
	60-165	26	122	1.7	2.8
3	BiP 5′NCR	50	55	1	1
	X-N	58	60	1.1	1.1
	S-N	61	60	1.2	1.1
	Xba	100	1000[b]	2	18
	Sma	103	ND	2	ND
	X-S	503[b]	650[b]	10	11

[a]The concentration needed to abolish 50% of p95–BiP 5′NCR complexes is shown. Note that the amount of full-length BiP 5′NCR needed to compete for 50% of p95–BiP 5′NCR complexes varies in different extracts. This is likely to be due to different concentrations of p95 and p60 in the extracts.
[b]Data point was obtained by extrapolation.
ND, not determined.

Next, we tested whether the complexes formed between p95 or p60 and the full-length BiP 5′NCR sequences could be competed by the smaller RNAs. Table 1 summarizes the results obtained in competition experiments using BiP 5′NCR–p95 and BiP 5′NCR–p60 complexes. Fragments containing the 3′ half of the BiP 5′NCR (X-N, S-N, delN-S and delN-H) abolished binding of p95 to the BiP 5′NCR with efficiencies comparable to that of the entire 5′NCR. Consistent with the results of the direct binding experiments (Fig. 5A), fragments containing the 5′ half of the BiP 5′NCR did not abolish the formation of BiP 5′NCR–p95 complexes readily (e.g. Nru and X-S). Fragments 60–165 and Sma (1–129) competed with the formation of BiP IRES–p95 complexes at higher concentrations, indicating that these RNAs contain a weak p95 binding site. Sequences encoded in the Xba (1–91) fragment competed to the same degree as the Sma sequences (1–129) for the formation of BiP IRES–p95 complexes. This was surprising because p95 could not be efficiently crosslinked to labeled Xba-RNA sequences (Fig. 5A, lane 3). The reason for this discrepancy is not clear.

Table 1 also displays the data obtained from BiP 5′NCR–p60 competition experiments. Again, as was observed in the direct binding experiments, fragments representing the 3′ half of the BiP 5′NCR (X-N, S-N, H-N del N-S) competed for formation of BiP 5′NCR–p60 complexes efficiently, while fragments containing the 5′ half of the BiP 5′NCR (Nru, X-S, Xba) and fragment 60–165 did not compete well.

Overall, the strongest binding sites for both p95 and p60 reside in the 3′ half (nt 129–220) of the BiP 5′NCR. In contrast to p60, p95 seems to have a weak binding site in RNA fragments containing sequences 1–91 (Xba), 1–129 (Sma) and 60–165. Whether p95 and p60 occupy the identical binding site between nt 129 and 220 remains to be determined.

Interaction of p95 and p60 with viral IRES elements

To test for an interaction of p95 with viral IRES elements, partially purified extracts were incubated with radiolabeled, thio-uridine containing IRES elements from the 5′NCRs of BiP, encephalomyocarditis virus (EMCV) (6) and poliovirus (POLIO) (5), respectively. After irradiation, crosslinked RNA–protein complexes were separated in SDS–polyacrylamide gels. Figure 6A shows that both the BiP 5′NCR (lane 2) and viral IRES elements (lanes 3 and 4) could be crosslinked to a 95 000 molecular weight protein. Many proteins could be crosslinked to the various viral IRES elements (lanes 3 and 4). This finding is not too surprising because the viral IRES elements, ~600 nt in length, have been shown to interact with numerous cellular proteins (reviewed in 3). However, the 95 kDa protein did not crosslink efficiently to the 5′NCR of globin mRNA (lane 1). To determine whether the 95 kDa viral IRES binding protein is identical to the BiP 5′NCR–p95 binding protein, competition studies were performed. Figure 6B shows that the formation of BiP 5′NCR–p95 complexes was inhibited in reactions containing 1 nM radiolabeled BiP substrate RNA and 12 nM of unlabeled cellular BiP 5′NCR (lane 2), or viral EMCV (lanes 3) and hepatitis C virus (HCV) (29,42) (lane 4) IRES elements. Similarly, addition of unlabeled polioviral IRES elements inhibited the formation of BiP IRES–p95 complexes (not shown). However, addition of similar amounts of IRE RNA did not abolish the formation of BiP 5′NCR–p95 complexes (lane 5). Thus, the same 95 kDa binds to the cellular BiP and to the viral EMCV, HCV and polioviral IRES elements.

Lastly, the affinity of p60 to cellular BiP 5′NCR and viral IRES elements was tested. Partially purified extracts containing p60 were directly crosslinked to BiP, EMCV, poliovirus and HCV IRES elements, respectively. Figure 6C shows that p60 was the predominant protein that could be crosslinked to the BiP IRES (lane 1). Many proteins, including a 60 kDa protein, were crosslinked to the viral IRES elements (lanes 2–4). In contrast, very little 60 kDa protein could be crosslinked to the same amount of globin 5′NCR (lane 5) or P4 RNA (lane 6), labeled to the same specific activity. Competition experiments showed that the formation of BiP IRES–p60 complexes could be abolished by the addition of excess cellular BiP 5′NCR (lane 8) or viral (lanes 9 and 10) IRES elements, but the formation of nucleoprotein complexes was unaffected by the presence of excess IRE (lane 11) or P4 (lane 12) RNAs.

These findings indicate that the same cellular proteins, p95 and p60, interact with both the cellular BiP 5′NCR and several viral IRES elements.

DISCUSSION

Expression of various dicistronic mRNAs which contained various parts of the 5′NCR of BiP mRNA in their intracistronic spacer regions revealed that the BiP IRES is located in the 3′ end of the NCR encompassing nt 129–220. Interestingly, using a combination of computer-aided thermodynamic, phylogenetic and statistical methods, Le and Maizel (39) identified a 92 nt unusual folding region (UFR) in the BiP 5′NCR spanning nt 129–220. The structure of the UFR could be folded into a Y-type stem–loop with an additional hairpin located immediately

upstream of the start-site AUG codon (39). The UFR was predicted to be present in human, hamster, rat, *Saccharomyces cerevisiae*, *Caenorhabditis elegans*, *Trypanosoma brucei* and *Giardia lamblia* BiP mRNAs (39), suggesting that the structure of the UFR has a conserved function. Interestingly, the IRES located in human fibroblast growth factor 2 (11) is predicted to contain a similar UFR element located immediately upstream of the translation start codon (39), indicating that the UFR may be a common motif in cellular IRES elements. However, compared to these cellular IRES elements, the folding of viral IRES elements predicts a somewhat more complex structure (43–46).

Although several cellular and viral IRES elements have been identified to date, only a few factors have been shown to be important in ribosomal subunit recruitment. Besides the translation initiation factors eIF-4A and cleaved eIF-4G, two predominantly nuclear RNA binding proteins, the La autoantigen (18,19) and the polypyrimidine tract binding protein PTB (20,21) are the only proteins thus far shown to have effects on efficient internal ribosome entry in certain viral IRES elements (22–24). However, neither La nor PTB interacts with the cellular BiP IRES.

We searched for RNA binding proteins that interact specifically with the BiP 5′NCR. Using ultraviolet crosslinking assays, p95 and p60 proteins that specifically bound to the BiP 5′NCR were identified. It is interesting that the p95 and p60 binding sites seem to overlap. It is not yet clear whether p95 and p60 are different proteins, or whether p60 represents a truncated version of p95; cloning the genes encoding p95 and p60 is in progress. p60 is not identical to La or PTB. First, immunoprecipitation of extracts with antibodies directed against either La or PTB identified La and PTB proteins that migrated differently than p60 in SDS–polyacrylamide gels (data not shown). And secondly, p60–BiP IRES complexes were not immunoprecipitated with either serum, and preincubation of extracts with either serum did not abolish the formation of p60–BiP IRES complexes (data not shown).

The observation that p95 and p60 bound to the BiP 5′NCR and several viral IRES elements makes them good candidates for being involved in translational regulation. Proof for this hypothesis awaits the rigorous purification of p60 and p95; the effects of purified proteins on the translation of BiP and IRES-containing viral RNAs can then be tested in cell-free translation systems.

ACKNOWLEDGEMENTS

We thank Karla Kirkegaard for valuable discussions and critical reading of the manuscript. This work was supported by The Council for Tobacco Research, USA and by grant AG07347 from the National Institutes of Health. P.S. acknowledges the receipt of a Faculty Research Award from the American Cancer Society.

REFERENCES

1 Kozak, M. (1989) *J. Cell. Biol.*, **108**, 229–241.
2 Merrick, W. C. (1992) *Microbiol. Rev.*, **56**, 291–315.
3 Jackson, R. J. and Kaminski, A. (1995) *RNA*, **1**, 985–1000.
4 Jackson, R. J., Hunt, S. L., Reynolds, J. E. and Kaminski, A. (1995) *Curr. Top. Microbiol. Immunol.*, **203**, 1–29.
5 Pelletier, J. and Sonenberg, N. (1988) *Nature*, **334**, 320–325.
6 Jang, S. K., Krausslich, H. G., Nicklin, M. J. H., Duke, G. M., Palmenberg, A. C. and Wimmer, E. (1988) *J. Virol.*, **62**, 2636–2643.
7 Wimmer, E., Hellen, C. U. T. and Cao, X. (1993) *Annu. Rev. Genet.*, **27**, 353–436.
8 Etchison, D., Milburn, S. C., Edery, I., Sonenberg, N. and Hershey, J. W. B. (1982) *J. Biol. Chem.*, **257**, 14806–14810.
9 Macejak, D. G. and Sarnow, P. (1991) *Nature*, **353**, 90–94.
10 Oh, S. K., Scott, M. P. and Sarnow, P. (1992) *Genes Dev.*, **6,** 1643–1653.
11 Vagner, S., Gensac, M.-C., Maret, A., Bayard, F., Amalric, F., Prats, H. and Prats, A.-C. (1995) *Mol. Cell. Biol.*, **15**, 35–44.
12 Teerink, H., Voorma, H. O. and Thomas, A. A. (1995) *Biochim. Biophys. Acta*, **1264**, 403–408.
13 Gan, W. and Rhoads, R. E. (1996) *J. Biol. Chem.*, **271**, 623–626.
14 Pause, A., Methot, N., Svitkin, Y., Merrick, W. C. and Sonenberg, N. (1994) *EMBO J.*, **13**, 1205–1215.
15 Lamphear, B. J., Kirchweger, R., Skern, T. and Rhoads, R. E. (1995) *J. Biol. Chem.*, **270**, 21975–21983.
16 Ohlmann, T., Rau, M., Pain, V. M. and Morley, S. J. (1996) *EMBO J.*, **15**, 1371–1382.
17 Ohlmann, T., Rau, M., Morley, S. J. and Pain, V. M. (1995) *Nucleic Acids Res.*, **23**, 334–340.
18 Tan, E. M. (1989) *Adv. Immunol.*, **44**, 93–151.
19 Gottlieb, E. and Steitz, J. A. (1989) *EMBO J.*, **8**, 851–861.
20 Patton, J. G., Mayer, S. A., Tempst, P. and Nadal-Ginard, B. (1991) *Genes Dev.*, **5**, 1237–1251.
21 Gil, A., Sharp, P. A., Jaminson, S. F. and Garcia-Blanco, M. A. (1991) *Genes Dev.*, **5**, 224–236.
22 Meerovitch, K., Svitkin, Y. V., Lee, H. S., Lejbkowicz, F., Kenan, D. J., Chan, E. K. L., Agol, V. I., Keene, J. D. and Sonenberg, N. (1993) *J. Virol.*, **67**, 3798–3807.
23 Hellen, C. U. T., Witherell, G. W., Schmid, M., Shin, S. H., Pestova, T. V., Gil, A. and Wimmer, E. (1993) *Proc. Natl. Acad. Sci. USA*, **90**, 7642–7646.
24 Kaminski, A., Hunt, S. L., Patton, J. G. and Jackson, R. J. (1995) *RNA*, **1**, 924–938.
25 Macejak, D. G., Hambidge, S. J., Najita, L. M. and Sarnow, P. (1990) In Brinton, M. A. and Heinz, F. X. (eds), *New Aspects of Positive-Stranded RNA Viruses*. American Society for Microbiology, Washington, DC, pp. 152–157.
26 Ausubel, F. M., Brent, R., Kingston, R. E., Moore, D. D., Seidman, J. G., Smith, J. A. and Struhl, K. (1994) *Current Protocols in Molecular Biology*. Greene Publishing Associates, Inc. John Wiley and Sons, Inc., New York.
27 De Wet, J. R., Wood, K. V., DeLuca, M., Helinski, D. R. and Subramani, S. (1987) *Mol. Cell. Biol.*, **7**, 725–737.
28 McBratney, S. and Sarnow, P. (1996) *Mol. Cell. Biol.*, **16**, 3523–3534.
29 Tsukiyama-Kohara, K., Iizuka, N., Kohara, M. and Nomoto, A. (1992) *J. Virol.*, **66**, 1476–1483.
30 Chen, C. Y. and Sarnow, P. (1995) *Science (Washington DC)*, **268**, 415–417.
31 Sarnow, P. (1989) *Proc. Natl. Acad. Sci. USA*, **86**, 5795–5799.
32 Dignam, J. D., Lebovitz, R. M. and Roeder, R. G. (1983) *Nucleic Acids Res.*, **11**, 1475–1489.
33 Dignam, J. D., Martin, P. L., Shastry, B. S. and Roeder, R. G. (1983) *Methods Enzymol.*, **101**, 582–598.
34 Englard, S. and Seifert, S. (1990) In Deutscher, M. P. (ed.), *Methods in Enzymology: Guide to Protein Purification*. Academic Press Inc., San Diego, Vol. 182, pp. 285–300.
35 Ting, J. and Lee, A. S. (1988) *DNA*, **7**, 275–286.
36 Sagliocco, F. A., Vega Laso, M. R., Zhu, D., Tuite, M. F., McCarthy, J. E. and Brown, A. J. (1993) *J. Biol. Chem.*, **268**, 26522–26530.
37 Peabody, D. S. and Berg, P. (1986) *Mol. Cell. Biol.*, **6**, 2695–2703.
38 Iizuka, N., Chen, C., Yang, Q., Johannes, G. and Sarnow, P. (1995) In Sarnow, P. (ed.), *Current Topics in Microbiology and Immunology 203: Cap-Independent Translation*. Springer Verlag, Berlin, pp. 155–177.
39 Le, S.-Y. and Maizel, J. V., Jr (1997) *Nucleic Acids Res.*, **25**, 362–369.
40 Hentze, M. W., Rouault, T. A., Caughman, S. W., Dancis, A., Harford, J. B. and Klausner, R. D. (1987) *Proc. Natl. Acad. Sci. USA*, **84**, 6730–6734.
41 Hentze, M. W. (1994) *Adv. Exp. Med. Biol.*, **356**, 119–126.
42 Wang, C., Sarnow, P. and Siddiqui, A. (1993) *J. Virol.*, **67**, 3338–3344.
43 Le, S. Y., Chen, J. H., Sonenberg, N. and Maizel, J. V. (1992) *Virology*, **191**, 858–866.
44 Le, S. Y. and Zuker, M. (1990) *J. Mol. Biol.*, **216**, 729–741.
45 Le, S. Y., Chen, J. H., Sonenberg, N. and Maizel, J. V., Jr (1993) *Nucleic Acids Res.*, **21**, 2445–2451.
46 Le, S. Y., Sonenberg, N. and Maizel, J. V., Jr (1995) *Gene*, **154**, 137–143.